



## Gaussian distribution of inhomogeneous barrier height in Ag/p-Si (1 0 0) Schottky barrier diodes

S. Acar<sup>a,\*</sup>, S. Karadeniz<sup>b</sup>, N. Tuğluoğlu<sup>b</sup>, A.B. Selçuk<sup>b</sup>, M. Kasap<sup>a</sup>

<sup>a</sup>Department of Physics, Faculty of Arts and Sciences, Gazi University, 06500 Ankara, Turkey

<sup>b</sup>Department of Materials Research, Ankara Nuclear Research and Training Center, Beşevler, 06100 Ankara, Turkey

Accepted 1 April 2004

Available online 28 May 2004

### Abstract

The current–voltage ( $I$ – $V$ ) measurements on Ag/p-Si Schottky barrier diodes in the temperature range 125–300 K were carried out. The  $I$ – $V$  analysis based on the thermionic emission (TE) theory has revealed an abnormal decrease of apparent barrier height and increase of ideality factor at low temperature. It is demonstrated that these anomalies result due to the barrier height inhomogeneities prevailing at the metal–semiconductor interface. A  $\Phi_{b0}$  versus  $q/2kT$  plot was drawn to obtain evidence of a Gaussian distribution of the barrier heights, and values of  $\Phi_{b0} = 0.780$  eV and  $\sigma_{s0} = 0.0906$  V for the mean barrier height and standard deviation at zero bias have been obtained from this plot, respectively. Furthermore, the mean barrier height and the Richardson constant values were obtained as 0.773 eV and  $15.53 \text{ A K}^{-2} \text{ cm}^{-2}$ , respectively, by means of the modified Richardson plot,  $\ln(I_0/T^2) - (q^2\sigma_{s0}^2/2k^2T^2)$  versus  $1000/T$ . Thus, it has been concluded that the temperature dependence of the  $I$ – $V$  characteristics of the Schottky barrier on p-type Si can be successfully explained on the basis of thermionic emission mechanism with Gaussian distribution of the barrier heights. Moreover, the value of the Richardson constant was found to be  $15.53 \text{ A K}^{-2} \text{ cm}^{-2}$ , which is close to the theoretical value of  $32 \text{ A K}^{-2} \text{ cm}^{-2}$  used for the determination of the zero-bias barrier height.

© 2004 Elsevier B.V. All rights reserved.

PACS: 73.30.+y; 73.40.Ns

Keywords: Metal–semiconductor contact; Gaussian distribution; Barrier height inhomogeneity

### 1. Introduction

Schottky barriers formed by metal–semiconductor contact have been widely studied in the past 60 years [1–3]. Due to the technological importance of Schottky barrier diodes, a full understanding of the nature of their current–voltage ( $I$ – $V$ ) and capacitance–

voltage ( $C$ – $V$ ) characteristics is of greater interest [3–32]. The most important feature characterizing a Schottky barrier is its barrier height  $\Phi_b$ . Several theories exist, which however can explain only some of the experimental facts. Therefore, there is a need for new experiments, which may yield more insight into the mechanisms determining  $\Phi_b$ . The spatial variation of barrier heights in inhomogeneous Schottky diodes is described mainly by the Gaussian distribution function. In the past, the Gaussian distribution of

\* Corresponding author. Tel.: +90-312-212-60-30.

E-mail address: [sacar@gazi.edu.tr](mailto:sacar@gazi.edu.tr) (S. Acar).

barrier heights has been widely accepted to correlate experimental data [3–20]. The ballistic electron emission microscopy (BEEM) studies have also supported the existence of Gaussian distribution of barrier heights in Schottky diodes [21,22]. Simulation studies on  $I$ – $V$  characteristics of inhomogeneous diodes with a Gaussian distribution of barrier heights have also yielded results similar to those observed in experimental data [11,23,24]. Analysis of the  $I$ – $V$  characteristics of Schottky barrier diodes based on thermionic emission theory usually reveals an abnormal decrease in the barrier height  $\Phi_b$  and an increase in the ideality factor  $n$  with decreasing temperature [3–20]. The decrease in the barrier height at low temperatures leads to non-linearity in the activation energy  $\ln(I_0/T^2)$  versus  $1/T$  plot. Nowadays, the nature and origin of the decrease in the barrier height and increase in ideality factor with a decrease in temperature in some studies [3–20] have been successfully explained on the basis of a thermionic emission mechanism with Gaussian distribution of the barrier heights.

In this report, we present  $I$ – $V$ – $T$  measurements in the temperature range 125–300 K on inhomogeneous Ag/p-Si Schottky barrier diodes. The temperature dependence of the barrier height and the ideality factor is discussed using TE theory with Gaussian distribution of the barrier heights around a mean value due to barrier height inhomogeneities prevailing at the metal–semiconductor interface.

## 2. Experimental

The semiconductor substrates used in this work were p-type B-doped Si single crystals, with a (1 0 0) surface orientation, 280  $\mu\text{m}$  thick and 0.8  $\Omega\text{ cm}$  resistivity. Before making contacts, the Si wafer was degreased for 5 min in boiling trichloroethylene, acetone and ethanol, consecutively. The wafer was chemically cleaned using the RCA cleaning procedure (i.e. a 10 min boil in  $\text{NH}_3 + \text{H}_2\text{O}_2 + 6\text{H}_2\text{O}$  followed by a 10 min boil in  $\text{HCl} + \text{H}_2\text{O}_2 + 6\text{H}_2\text{O}$ ) with the final dip in diluted HF for 30 s, and then rinsed in deionized water of resistivity of 18 M $\Omega\text{ cm}$  with ultrasonic vibration and dried by high purity nitrogen. Immediately after surface cleaning, high purity aluminum (Al) metal (99.999%) with a thickness of 2000 Å was thermally evaporated from the

tungsten filament onto the whole back surface of the wafer in the pressure of  $1 \times 10^{-7}$  Torr. Then, a low resistivity ohmic contact was followed by a temperature treatment at 500 °C for 3 min in  $\text{N}_2$  atmosphere. The Schottky contacts were formed on the other faces by evaporating silver (Ag, 99.999%) with a thickness of 1500 Å as dots with diameter of about 1.0 mm (diode area =  $176 \times 10^{-2}\text{ cm}^2$ ) through a metal shadow mask in liquid nitrogen trapped high vacuum system in the pressure of  $1 \times 10^{-7}$  Torr. Metal layer thickness as well as deposition rates were monitored with the help of a digital quartz crystal thickness monitor. The deposition rates were about 10–20 Å/s.

The  $I$ – $V$  measurements were performed by the use of a Keithley 220 programmable constant current source, a Keithley 614 electrometer. The  $C$ – $V$  measurements were performed at 1 MHz by using HP 4192A LF impedance analyzer (5 Hz to 13 MHz). The  $I$ – $V$  and  $C$ – $V$  characteristics of the Ag/p-Si Schottky diode were studied in the temperature range of 125–300 K by using temperature controlled Janes vp-475 cryostat.

## 3. Results and discussion

### 3.1. Forward-bias $I$ – $V$ characteristics of Ag/p-Si Schottky barrier diodes

For a Schottky barrier diode, current transport is due to majority carriers and it may be described by thermionic emission (TE) over the interface barrier. TE current at the forward bias can be written as [1]:

$$I = I_0 \exp\left(\frac{qV}{nkT}\right) \left[1 - \exp\left(-\frac{qV}{kT}\right)\right] \quad (1)$$

where  $n$  is the ideality factor,  $I_0$  the saturation current and defined by

$$I_0 = AA^*T^2 \exp\left[-\frac{q\Phi_{b0}}{kT}\right] \quad (2)$$

where the quantities  $A$ ,  $A^*$ ,  $T$ ,  $q$ ,  $k$  and  $\Phi_{b0}$  are the diode area, the effective Richardson constant of 32 A K $^{-2}\text{ cm}^{-2}$  for p-type Si, temperature in K, the electronic charge, Boltzmann's constant and the zero-bias barrier height, respectively. Fig. 1 shows the semilog  $I$ – $V$  characteristics of the Ag/p-Si Schottky diodes at different temperatures. We have performed

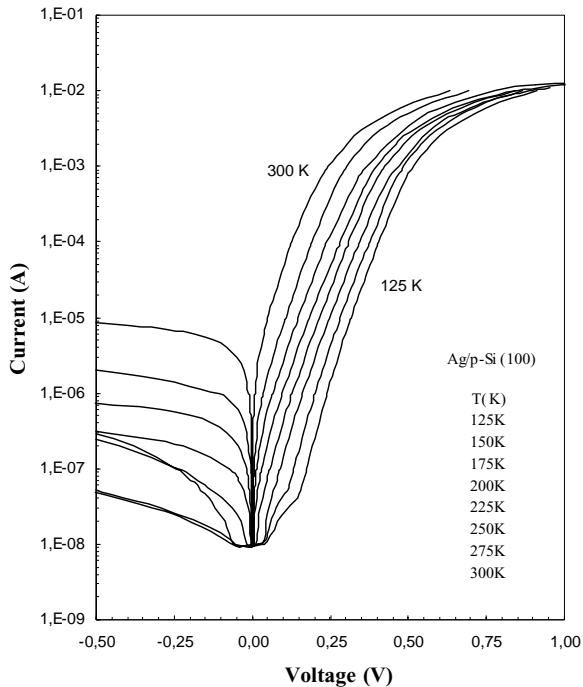


Fig. 1. Experimental forward-bias current–voltage characteristics of Ag/p-Si Schottky diode at different temperatures.

least square fits of Eq. (1) to the linear part of the measured  $I$ – $V$  plots (Fig. 1). From these fits, the experimental values of  $n$  and  $\Phi_{b0}$  were determined from intercepts and slopes of the forward bias  $\ln I$  versus  $V$  plot at each temperature, respectively. Once  $I_0$  is known, the zero bias barrier height can be computed with the help of Eq. (2). The  $\Phi_{b0}$  and  $n$  determined from semilog-forward  $I$ – $V$  plots were found to be a strong function of temperature. The ideality factor  $n$  was found to increase, while the  $\Phi_{b0}$  decrease with decreasing temperature, as can be seen in Figs. 2 and 3, respectively ( $n = 2.25$  and  $\Phi_{b0} = 0.398$  eV at 125 K,  $n = 1.35$  and  $\Phi_{b0} = 0.619$  eV at 300 K). The values of  $\Phi_{b0}$  (indicated by open circles) and  $\Phi_{CV}$  (indicated by open squares) obtained from the forward bias  $I$ – $V$  and the reverse bias  $C^{-2}$ – $V$  characteristics (Fig. 4) depending on the temperature are given in Fig. 3. As explained in [10–12], since current transport across the metal–semiconductor interface is a temperature activated process, electrons at low temperatures are able to surmount the lower barriers and therefore current transport will be dominated by current flowing through patches of the lower Schottky

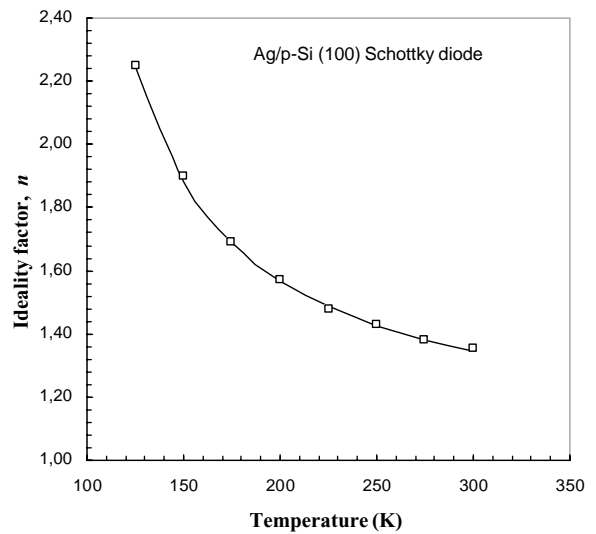


Fig. 2. Temperature dependence of the ideality factor for Ag/p-Si Schottky diode in the range 100–300 K. The continuous curve shows the estimated value of the ideality factor using Eq. (11) with  $\rho_2 = -0.0437$  V and  $\rho_3 = 0.011$  V.

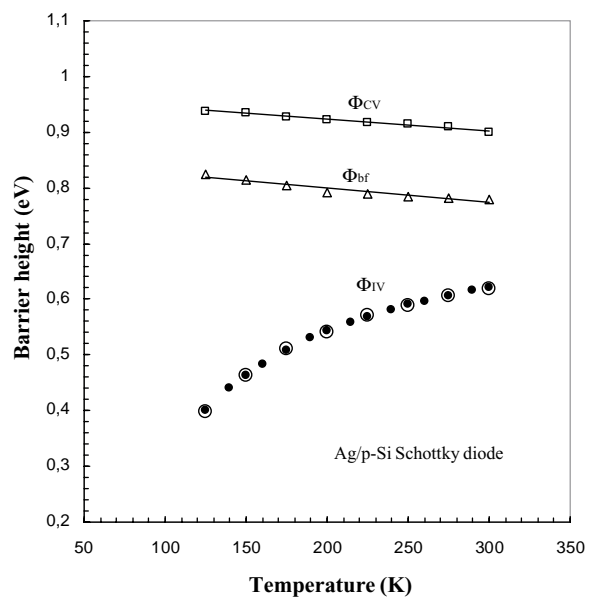


Fig. 3. Temperature dependence of the zero-bias apparent barrier height and flat-band barrier height for Ag/p-Si Schottky diode. The solid circles represent estimated values of  $\Phi_{ap}$  using Eq. (10) with  $\bar{\Phi}_{b0} = 0.780$  eV and  $\sigma_{s0} = 0.0906$  V values.

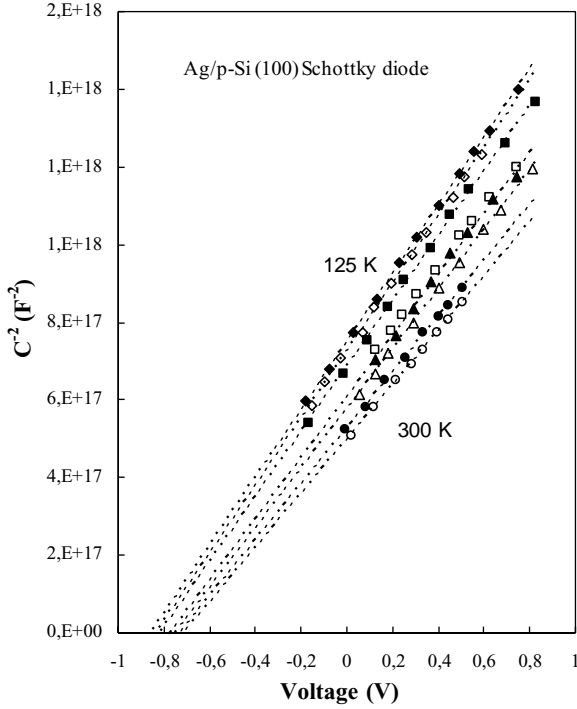


Fig. 4. Experimental reverse bias  $C^{-2}$ – $V$  characteristics of Ag/p-Si Schottky diode at various temperatures.

barrier height and a larger ideality factor. As the temperature increases, more and more electrons have sufficient energy to surmount the higher barrier. As a result, the dominant barrier height will increase with the temperature and bias voltage.

For the evaluation of the barrier height, one may also make use of the Richardson plot of the saturation current. Eq. (2) can be rewritten as

$$\ln\left(\frac{I_0}{T^2}\right) = \ln(AA^*) - \frac{q\Phi_{b0}}{kT} \quad (3)$$

The dependence of  $\ln(I_0/T^2)$  versus  $1000/T$  is found to be non-linear in the temperature range measured; however, the dependence of  $\ln(I_0/T^2)$  versus  $1000/nT$  gives a straight line (Fig. 5). The non-linearity of the conventional  $\ln(I_0/T^2)$  versus  $1000/T$  is caused by the temperature dependence of the barrier height and ideality factor. Similar results have also been found by several authors [10–20]. The experimental data are seen to fit asymptotically to a straight line at higher temperatures only. An activation energy value of 0.420 eV from the slope of this straight line was

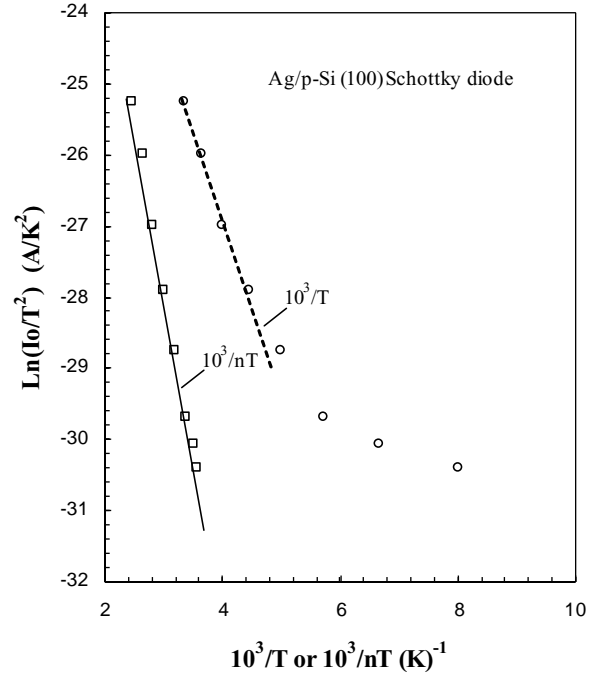


Fig. 5. Richardson plots of  $\ln(I_0/T^2)$  vs.  $10^3/T$  or  $10^3/nT$  for Ag/p-Si Schottky diode.

obtained for the device. As will be discussed below, the deviation in the Richardson plots may be due to the spatially inhomogeneous barrier heights and potential fluctuations at the metal–semiconductor interface that consist of low and high barrier areas [6–17], that is, the current through the diode will flow preferentially through the lower barriers in the potential distribution [6–17]. The values of  $A^*$  obtained from the intercept of the straight portion at the ordinate of the experimental  $\ln(I_0/T^2)$  versus  $1000/T$  and  $\ln(I_0/T^2)$  versus  $1000/nT$  plot in Fig. 5 are equal to  $1.04 \times 10^{-3} \text{ A K}^{-2} \text{ cm}^{-2}$  and  $0.056 \text{ A K}^{-2} \text{ cm}^{-2}$ , respectively. The value of  $A^*$  for holes in p-type Si is much lower than both the theoretically calculated ( $32 \text{ A K}^{-2} \text{ cm}^{-2}$  for holes in p-type Si). Horváth [25] explained that the  $A^*$  value obtained from the temperature dependence of the  $I$ – $V$  characteristic may be affected by lateral inhomogeneity of the barrier.

According to [10–12,18–20], the ideality factor of an inhomogeneous Schottky barrier diode with a distribution of low Schottky barrier heights may increase with a decrease in temperature. The

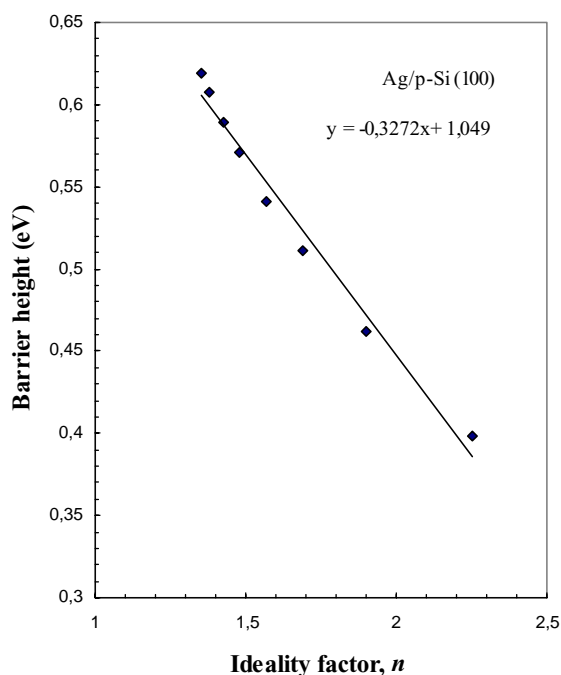


Fig. 6. Zero-bias apparent barrier height vs. ideality factor of a typical Ag/p-Si Schottky diode at different temperatures.

Schottky barrier consists of laterally inhomogeneous patches of different barrier heights. Schmitsdorf et al. [19] used Tung's theoretical approach and they found a linear correlation between the experimental zero-bias Schottky barrier heights and ideality factors. We prepared a plot of the experimental barrier height versus the ideality factor (Fig. 6). The straight line in Fig. 6 is the least squares fit to the experimental data. As can be seen from Fig. 6, there is a linear relationship between the experimental effective barrier heights and the ideality factors of the Schottky contact that was explained by lateral inhomogeneities of the barrier heights in the Schottky diodes [14–20]. The extrapolation of the experimental barrier heights versus ideality factor plot to  $n = 1$  has given a homogeneous barrier height of approximately 0.722 eV. Thus, it can be said that the significant decrease of the zero-bias barrier height and increase of the ideality factor especially at low temperature are possibly caused by the barrier inhomogeneities.

The barrier height, which decreases with decreasing temperature, obtained from Eq. (2) is called apparent

or zero-bias barrier height. The barrier height obtained under flat-band condition is called flat-band barrier height and is considered to be real fundamental quantity. Unlike the case of the zero-bias barrier height, the electrical field in the semiconductor is zero under the flat-band condition. This eliminates the effect of the image force lowering that would affect the  $I$ – $V$  characteristics and removes the influence of lateral inhomogeneity [10,27]. To find out the value of  $\Phi_{bf}$  use is made of the expression [28,29]:

$$\Phi_{bf} = n\Phi_{b0} - (n - 1) \left( \frac{kT}{q} \right) \ln \left( \frac{N_v}{N_A} \right) \quad (4)$$

where  $N_v$  is the effective density of states in the valance band and  $N_A$  the carrier concentration. The  $C$ – $V$  measurements have been performed at 1 MHz in the temperature range of 125–300 K. The experimental  $N_A$  and  $N_v$  depending on the temperature were calculated from the reverse bias  $C^{-2}$ – $V$  characteristics in Fig. 4. The values of  $N_A$  and  $N_v$  are  $1.35 \times 10^{16} \text{ cm}^{-3}$  at 125 K and  $1.73 \times 10^{16} \text{ cm}^{-3}$  at 300 K, and  $2.74 \times 10^{18} \text{ cm}^{-3}$  at 125 K and  $1.02 \times 10^{19} \text{ cm}^{-3}$  at 300 K, respectively. The  $N_A$  and  $N_v$  of the p-Si decreased slightly with a decrease in temperature in the temperature range of 125–300 K. Fig. 3 shows the variation of  $\Phi_{bf}$  as a function of the temperature.  $\Phi_{bf}$  is always larger than zero-bias barrier height  $\Phi_{b0}$  and appears at first glance to be nearly constant with a slight variation. However, the flat-band barrier height  $\Phi_{bf}$  is obtained to increase with decreasing temperature in a manner similar to those reported by the others [13,26–29]. Furthermore, the temperature dependence of the flat-band barrier height can be expressed as

$$\Phi_{bf}(T) = \Phi_{bf}(T = 0) + \alpha T \quad (5)$$

where  $\Phi_{bf}(T = 0)$  is the zero-temperature flat-band barrier height and  $\alpha$  is the temperature coefficient of  $\Phi_{bf}$ . A plot of the flat-band barrier height  $\Phi_{bf}$  as a function of the temperature is shown Fig. 3 (indicated by open triangles). In Fig. 3, the fitting of  $\Phi_{bf}(T)$  data in Eq. (4) yields  $\Phi_{bf}(T = 0) = 0.850 \text{ eV}$  and  $\alpha = -0.256 \text{ meV K}^{-1}$ . In the same way, in Fig. 3 (indicated by open squares), the experimental  $\Phi_{CV}$  versus  $T$  plot from the reverse bias  $C$ – $V$  data as a function of the temperature yields  $\Phi_{CV}(T = 0) = 0.965 \text{ eV}$  and  $\alpha = -0.212 \text{ meV K}^{-1}$ . The experimental values of the temperature coefficient of the barrier height for

the Ag/p-type Si Schottky barrier diode is in very close agreement with the temperature coefficient value of  $-0.24 \text{ meV K}^{-1}$  of the energy gap for Si given in [30–32]. It was reported the barrier height temperature coefficient value of  $-0.121 \text{ meV K}^{-1}$  for PtSi/p-Si by McCafferty et al. [4], values in the range of  $-0.128$  to  $-0.147 \text{ meV K}^{-1}$  for Ti/p-Si and TiSi<sub>2</sub>/p-Si by Aboelfotoh and Tu [30,31], values of  $-0.252$  and  $-0.326 \text{ meV K}^{-1}$  for PtSi/n-Si (1 0 0) Schottky barrier diodes by Werner and Güttler [7] and  $-0.126 \text{ meV K}^{-1}$  for PtSi/p-Si (1 0 0) Schottky barrier diodes in another paper [28].

### 3.2. The analysis of barrier height inhomogeneities

As first introduced by Song et al. [8], the above abnormal behaviors can be explained by using an analytical potential fluctuation model based on spatially inhomogeneous barrier heights at the interface [5–17,26]. Let us assume a Gaussian distribution of the barrier heights with a mean value  $\bar{\Phi}_b$  and a standard deviation  $\sigma_s$  in the form:

$$P(\Phi_b) = \frac{1}{\sigma_s \sqrt{2\pi}} \exp\left(-\frac{(\bar{\Phi}_b - \Phi_b)^2}{2\sigma_s^2}\right) \quad (6)$$

where  $1/\sigma_s \sqrt{2\pi}$  is the normalization constant. The total current  $I$  a forward bias  $V$  is given by

$$I(V) = \int_{-\infty}^{+\infty} I(\Phi_b, V) P(\Phi_b) d\Phi_b \quad (7)$$

On integration

$$I(V) = A^* T^2 \exp\left[-\frac{q}{kT} \left(\bar{\Phi}_b - \frac{q\sigma_s^2}{2kT}\right)\right] \times \exp\left(\frac{qV}{n_{ap} kT}\right) \left[1 - \exp\left(-\frac{qV}{kT}\right)\right] \quad (8)$$

with

$$I_0 = AA^* T^2 \exp\left(\frac{q\Phi_{ap}}{kT}\right) \quad (9)$$

where  $I_0$  is the saturation current, and  $\Phi_{ap}$  and  $n_{ap}$  the apparent barrier height and apparent ideality factor at zero bias, respectively:

$$\Phi_{ap} = \bar{\Phi}_{b0}(T=0) - \frac{q\sigma_{s0}^2}{2kT} \quad (10)$$

In the ideal case ( $n = 1$ ), the expression is obtained as the following suggested by

$$\left(\frac{1}{n_{ap}} - 1\right) = \rho_2 - \frac{q\rho_3}{2kT} \quad (11)$$

The temperature dependence of  $\sigma_s$  is usually small and thus can be neglected [9]. However, it is assumed that the standard deviation  $\sigma_s$  and the mean value of the Schottky barrier height  $\bar{\Phi}_b$  are the bias voltages linearly dependent on Gaussian parameters that are given by  $\bar{\Phi}_b = \bar{\Phi}_{b0} + \rho_2 V$  and  $\sigma_s = \sigma_{s0} + \rho_3 V$ , where  $\rho_2$  and  $\rho_3$  are the voltage coefficients that may depend on temperature ( $T$ ) and they quantify the voltage deformation of the barrier height distribution [9,10]. It is obvious that the decrease of zero-bias barrier height is caused by the existence of the Gaussian distribution and the extent of influence is determined by the standard deviation itself. Also, the effect is particularly significant at low temperatures. On the other hand, the abnormal increase of ideality factor occurs due to the variation of mean barrier height and standard deviation with bias, i.e., terms involving voltage coefficients  $\rho_2$  and  $\rho_3$ .

As Eqs. (2) and (9) are of the same form, the fitting of the experimental data to Eq. (2) gives  $\Phi_{ap}$  and  $n_{ap}$ , respectively, which should obey Eqs. (10) and (11). Thus, the plot of  $\Phi_{ap}$  versus  $1000/T$  should be a straight line giving  $\bar{\Phi}_{b0}$  and  $\sigma_{s0}$  from the intercept and slope, respectively. Fig. 7 shows this plot. The values of 0.780 eV and 0.0906 V for  $\bar{\Phi}_{b0}$  and  $\sigma_{s0}$ , respectively, were obtained from the least-square linear fitting of the data. Furthermore, as can be seen from Fig. 7, the experimental results of  $\Phi_{ap}$  fit very well with theoretical equation (10) denoted by closed circles, with the same parameters. When comparing  $\bar{\Phi}_{b0}$  and  $\sigma_{s0}$  parameters, it is seen that the standard deviation is  $\approx 11\%$  of the mean barrier height. The standard deviation is a measure of the barrier homogeneity. As the lower value of  $\sigma_{s0}$  corresponds to a more homogeneous barrier height, it indicates the larger inhomogeneities at the interface of our Ag/p-Si device. According to these results, as was reported in [7–9] barrier inhomogeneities can occur as a result of inhomogeneities in the composition of the interfacial oxide layer, non-uniformity of interfacial charges and interfacial oxide layer thickness.

The temperature dependence of the ideality factor can be understood on the basis of Eq. (11). Fitting

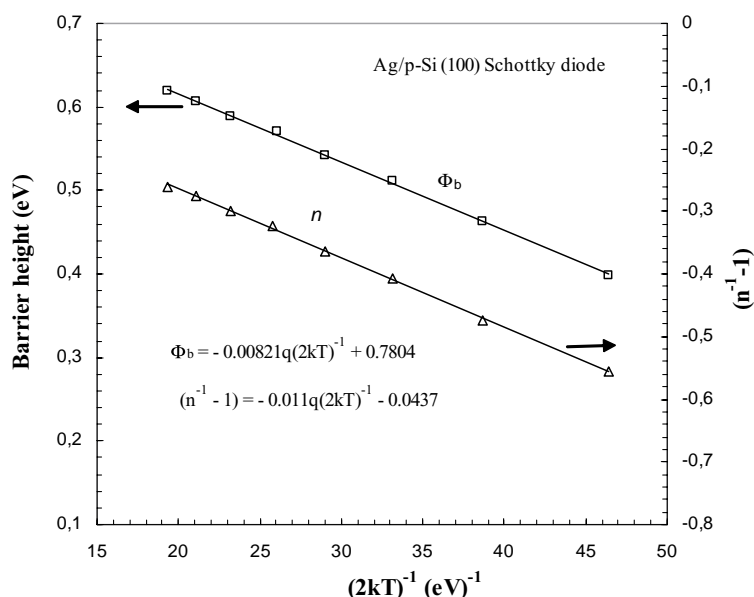


Fig. 7. Zero-bias apparent barrier height and ideality factor vs.  $1/T$  curves of Ag/p-Si Schottky diode according to Gaussian distribution of the barrier heights.

showing ideality factor  $n$  in Fig. 7 is a straight line that gives voltage coefficients  $\rho_2$  and  $\rho_3$  from the intercept and slope of the plot where  $\rho_2 = -0.0437$  V and  $\rho_3 = 0.011$  V from the experimental data. Furthermore, as can be seen from Fig. 7, the experimental results of  $n$  fit very well with the theoretical equation (11), denoted by solid line, with the same parameters. The linear behavior of the  $(1/n_{ap} - 1)$  versus  $q/2kT$  plot confirms that the ideality factor does indeed denote the voltage deformation of the Gaussian distribution of the barrier height. The continuous line in Fig. 2 represents data estimated with these parameters.

The Richardson plot is now modified by combining Eqs. (9) and (10):

$$\ln\left(\frac{I_0}{T^2}\right) - \left(\frac{q^2\sigma_{s0}^2}{2k^2T^2}\right) = \ln(AA^*) - \frac{q\bar{\Phi}_{b0}}{kT} \quad (12)$$

The modified  $\ln(I_0/T^2) - (q^2\sigma_{s0}^2/2k^2T^2)$  versus  $100/T$  plot according to Eq. (12) should also be a straight line with the slope and the intercept at the ordinate directly yielding the mean barrier height  $\bar{\Phi}_{b0}$  and  $A^*$ , respectively. Fig. 8 shows this plot. It can be seen that the modified Richardson plot has quite a good linearity over the whole temperature range corresponding to single activation energy around  $\bar{\Phi}_{b0}$ . By the least-squares linear fitting of the data,  $\bar{\Phi}_{b0} = 0.773$  eV

and  $A^* = 15.53 \text{ A cm}^{-2} \text{ K}^2$  are obtained. As can be seen, this value of  $\bar{\Phi}_{b0} = 0.773$  eV is in close agreement with the value of  $\bar{\Phi}_{b0} = 0.780$  eV from the plot

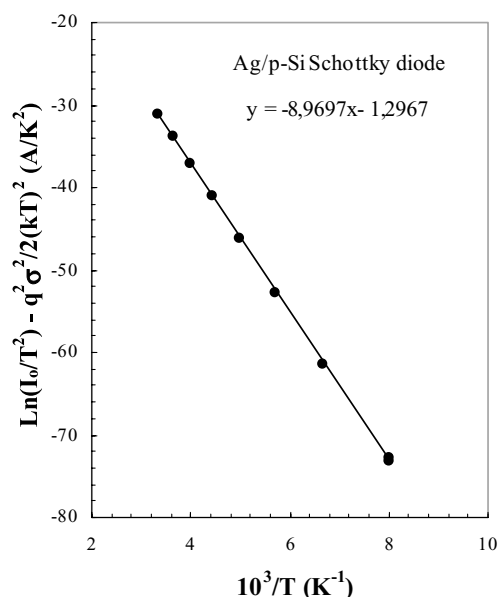


Fig. 8. Modified Richardson  $\ln(I_0/T^2) - (q^2\sigma_{s0}^2/2k^2T^2)$  vs.  $10^3/T$  plot for the Ag/p-Si Schottky diode according to Gaussian distribution of the barrier heights.



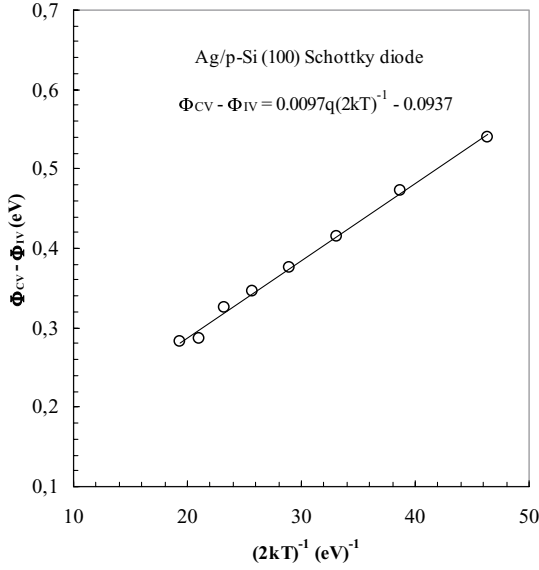


Fig. 9. The experimental  $(\Phi_{CV} - \Phi_{IV})$  vs.  $1/T$  curve of the Ag/p-Si Schottky diode according to Gaussian distribution of barrier heights in [7].

of  $\Phi_{ap}$  versus  $1000/T$  given in Fig. 7, while modified Richardson constant  $A^* = 15.53 \text{ A cm}^{-2} \text{ K}^2$  is in a closer agreement with the theoretical value of  $A^* = 32 \text{ A cm}^{-2} \text{ K}^2$  than the values of the  $A^*$  obtained in the previous section.

Moreover, it can be seen that the apparent barrier height from the experimental forward bias  $I$ - $V$  plot is also related to the mean barrier height  $\bar{\Phi}_b - \bar{\Phi}_{CV}$  from the experimental reverse bias  $C^{-2}$ - $V$  plot [7]. The capacitance depends only on the mean band bending and is insensitive to the standard deviation  $\sigma_s$  of the barrier distribution [7]. The relationship between  $\Phi_{ap}$  and  $\Phi_{CV}$  is given by [7]:

$$\bar{\Phi}_b - \Phi_{ap} = -\frac{q\sigma_0^2}{2kT} + \frac{q\alpha_\sigma}{2k} \quad (13)$$

where  $\alpha_\sigma$  is attributed to the temperature dependence of  $\sigma_s$ . Fig. 9 shows the experimental  $(\Phi_{CV} - \Phi_{IV})$  versus  $1/T$  plot according to Eq. (13). The plot should give a straight line of slope  $\sigma_0^2/2k$  and a y-axis intercept  $\alpha_\sigma/2k$  from which the parameters  $\sigma_0$  and  $\alpha_\sigma$  can be determined. The slope and y-axis intercept of the plot given the values of  $\sigma_0 = 0.098 \text{ V}$  and  $\alpha_\sigma = 16.163 \text{ mV}^2 \text{ K}^{-1}$ , respectively. This value of  $\sigma_0$  is in close agreement with the value of  $\sigma_0 = 0.0906 \text{ V}$  from the plot of  $\Phi_{ap}$  versus  $1/T$  drawn according to Eq. (10).

The case shows that Eq. (10) (the barrier height inhomogeneity model of Chand and Kumar [13] and Dobrocka and Osvald [24]) and Eq. (13) (the barrier height inhomogeneity model of Werner and Güttler [7] and Song et al. [8]) related to Gaussian distribution of the barrier heights with mean value  $\bar{\Phi}_b$  is in close agreement with each other.

#### 4. Conclusion

The current-voltage characteristics of Ag/p-Si Schottky contacts were measured in the temperature range 125–300 K. While the zero-bias barrier height  $\Phi_{b0}$  decrease, ideality factor  $n$  increases with a decrease in temperature; the changes are quite significant at low temperatures (below 200 K). Barrier height inhomogeneities at the interface cause deviation in the zero-bias barrier height and the ideality factor at low temperatures, and produce extra current such that the  $I$ - $V$  characteristics continue to remain consistent with the thermionic emission process. The inhomogeneities can be described by the Gaussian distribution of the barrier heights with mean barrier height  $\bar{\Phi}_{b0} = 0.780 \text{ eV}$  and standard deviation  $\sigma_{s0} = 0.0906 \text{ V}$ . The experimental results of  $\Phi_{ap}$  and  $n_{ap}$  fit very well with the theoretical equations related to the Gaussian distribution of  $\Phi_{ap}$  and  $n_{ap}$ . Moreover, the mean barrier height and the Richardson constant values were obtained as  $0.773 \text{ eV}$  and  $15.53 \text{ A K}^{-2} \text{ cm}^{-2}$ , respectively, by means of the modified Richardson plot,  $\ln(I_0/T^2) - (q^2\sigma_{s0}^2/2k^2T^2)$  versus  $1000/T$ . This value of the Richardson constant is in close agreement with the theoretical value of  $32 \text{ A K}^{-2} \text{ cm}^{-2}$  of holes in p-type Si. The difference of the Richardson constant from the theoretical may be connected with a value of the real effective mass. The most questionable parameter figuring in the tunneling theory in semiconductors is the effective mass of free carriers. It shows a behavior in both the tunneling probability and in the flux of carriers incident to the interface.

#### Acknowledgements

This work is supported by Turkish Atomic Energy Authority Supported Project “AP2 D1. Nuclear



Techniques in Sustainable Development and Environmental Protection” and DPT under Project No: 2001K120590.

## References

- [1] E.H. Rhoderick, R.H. Williams, *Metal–Semiconductor Contacts*, Clarendon Press, Oxford, 1988.
- [2] S.M. Sze, *Physics of Semiconductor Devices*, 2nd ed., Wiley, New York, 1981.
- [3] R.T. Tung, *Mater. Sci. Eng. R* 35 (2001) 1.
- [4] P.G. McCafferty, A. Sellai, P. Dawson, H. Elabd, *Solid-state Electron.* 39 (1996) 583.
- [5] A. Singh, K.C. Reinhardt, W.A. Anderson, *J. Appl. Phys.* 68 (1990) 3475.
- [6] S. Chand, J. Kumar, *Semicond. Sci. Technol.* 11 (1996) 1203.
- [7] J.H. Werner, H.H. Güttler, *J. Appl. Phys.* 69 (1991) 1522; H.H. Güttler, J.H. Werner, *Appl. Phys. Lett.* 56 (1990) 1113.
- [8] Y.P. Song, R.L. Van Meirhaeghe, W.F. Laflere, F. Cardon, *Solid-state Electron.* 29 (1986) 633.
- [9] S.Y. Zhu, R.L. Van Meirhaeghe, C. Detavernier, F. Cardon, G.P. Ru, X.P. Qu, B.Z. Li, *Solid-state Electron.* 44 (2000) 663.
- [10] A. Gümüş, A. Türit, N. Yalçın, *J. Appl. Phys.* 91 (2002) 245.
- [11] J.P. Sullivan, R.T. Tung, M.R. Pinto, W.R. Graham, *J. Appl. Phys.* 70 (1991) 7403.
- [12] R.T. Tung, *Appl. Phys. Lett.* 58 (1991) 2821; R.T. Tung, *Phys. Rev. B* 45 (1992) 13509.
- [13] S. Chand, J. Kumar, *J. Appl. Phys.* 80 (1996) 288; S. Chand, J. Kumar, *Appl. Phys. A* 63 (1996) 171.
- [14] Ş. Karataş, Ş. Altındal, A. Türit, A. Özmen, *Appl. Surf. Sci.* 217 (2003) 250.
- [15] S. Chand, *Semicond. Sci. Technol.* 17 (2002) L36.
- [16] S. Bandyopadhyay, A. Bhattacharya, S.K. Sen, *J. Appl. Phys.* 85 (1999) 3671.
- [17] B. Abay, G. Çankaya, H.S. Güder, H. Efeoğlu, Y.K. Yoğurtçu, *Semicond. Sci. Technol.* 18 (2003) 75.
- [18] C. Coşkun, M. Biber, H. Efeoğlu, *Appl. Surf. Sci.* 211 (2003) 360.
- [19] R.F. Schmitsdorf, T.U. Kampen, W. Mönch, *Surf. Sci.* 324 (1995) 249; W. Mönch, *J. Vac. Sci. Technol. B* 17 (1999) 1867.
- [20] M.K. Hudait, P. Venkateswarlu, S.B. Krupanidhi, *Solid-state Electron.* 45 (2001) 133.
- [21] G.M. Vanalme, L. Goubert, R.L. Van Meirhaeghe, F. Cardon, P.V. Daele, *Semicond. Sci. Technol.* 14 (1999) 871.
- [22] H. Palm, M. Arbes, M. Schulz, *Phys. Rev. Lett.* 71 (1993) 2224.
- [23] S. Chand, J. Kumar, *Semicond. Sci. Technol.* 12 (1997) 899.
- [24] E. Dobrocka, J. Osvald, *Appl. Phys. Lett.* 65 (1994) 575.
- [25] Zs.J. Horváth, *Solid-state Electron.* 39 (1996) 176.
- [26] F.E. Jones, B.P. Wood, J.A. Myser, C.H. Daniels, M.C. Lonergan, *J. Appl. Phys.* 86 (1999) 6431.
- [27] S. Hardikar, M.K. Hudait, P. Modak, S.B. Krupanidhi, N. Padha, *Appl. Phys. A* 68 (1999) 49.
- [28] J.H. Werner, H.H. Güttler, *J. Appl. Phys.* 73 (1993) 1315.
- [29] L.F. Wagner, R.W. Young, A. Sugerman, *IEEE Electron. Dev. Lett.* 4 (1983) 320.
- [30] M.O. Aboelfotoh, K.M. Tu, *Phys. Rev. B* 34 (1986) 2311.
- [31] M.O. Aboelfotoh, *J. Appl. Phys.* 64 (1988) 4046.
- [32] S. Zhu, R.L. Van Meirhaeghe, C. Detavernier, G.P. Ru, B.Z. Li, F. Cardon, *Solid-state Commun.* 112 (1999) 611.